Improving pore morphology of PM 316L stainless steels by prealloyed powder prepassivation in 20% nitric acid

B. Shahabi Kargar*, A. Babakhani and M. H. Moayed

The effect of prepassivation of prealloyed powder of 316L stainless steels on pore morphology and powder particle shape was investigated. Image analysis technique was used to study the effect of prepassivation, compaction and sintering temperature on the pore morphology of powder metallurgy 316L stainless steels. Porosity, dimension and morphology of the pores were characterised by means of four basic parameters: fraction of surface porosity, equivalent circle diameter, shape factor and elongation factor. In addition, SEM macrographs of powder particles were also investigated by applying the image analysis technique. The Feret's average diameter and elongation factor were employed to describe the size and roundness of powder particles respectively. Annealing treatment reduced the equivalent circle diameter of pores and simultaneously improved f_{shape} and f_{elong} towards higher values. It was proposed that the prepassivation treatment reduced irregularity of powder particles through elimination of sharp corners of powder particles by exposure to acid environment.

Keywords: Powder metallurgy, Pores morphology, Image analysis, Sintered stainless steel

Introduction

Powder metallurgy (PM) offers great advantages when manufacturing large series of small components with high tolerance and productivity. However, the use of PM stainless steels is often limited because of corrosion and mechanical properties lower than those of wrought materials. Differences of one or two orders of magnitude have been found between the corrosion rates i_{corr} of PM and wrought steels of similar composition (mainly depending on the processing parameters of PM stainless steels).[1–5]

Concerning stainless steels, the AISI 316L stainless steel powder is used to replace PM ferrous alloys due to its superior mechanical properties and corrosion resistance.[6] High strength sintered 316L stainless steel can be obtained by modification sintering process.[7] Strength increased as part density and sintering temperature increased. Additionally, to obtain a good combination of mechanical properties and corrosion resistance, steel compaction and sintering conditions must be optimised.[8]

Most of the properties of sintered components are strongly related to porosity, pores dimension and morphology.[9] The effect of porosity on mechanical properties depends on the following factors:

(i) the quantity of pores (i.e. the fractional porosity)
(ii) their interconnection
(iii) size
(iv) morphology
(v) distribution.[10]

In quantitative description of planar shape, two-dimensional shape parameters are used to compare the features of pores in PM products obtained with different materials and production techniques. To evaluate the pore characteristics, the image analysis techniques may be applied to the usual metallographic characterisation. Pores are clearly visible on an unetched metallographic section, and their morphology may be quantified by means of some shape factors.[11–13]

In this study, image analysis technique was used to study the effects of the process variables and prepassivation treatment on the pore morphology of PM 316L stainless steel. Both compaction and sintering were considered as process variables. In addition, SEM observation was applied to evaluate the powder particle characterisation. The effect of prepassivation treatment on the corrosion behaviour of samples was investigated separately, and the results were submitted for publication elsewhere.[14]

Experimental

A Höganäs prealloyed water atomised powder was used in this study: AISI 316LHD (0·025C–0·9Si–12·3Ni–16·7Cr–0·06N–0·1Mn–2·2Mo–0·005S–0·30O) with an apparent density of 2·67 g cm^{-3} (particle size, <75 μm). Prepassivation methods according to ASTM A967-01 were applied on powder particles using 20% nitric acid at 54°C and subsequently dried in an oven at 110°C after rinsing

Metallurgical and Materials Engineering Department, Ferdowsi University of Mashhad, Mashhad 91775–1111, Iran

*Corresponding author, email behzad892@gmail.com

Published by Maney on behalf of the Institute
Received 2 May 2010; accepted 25 August 2010
DOI 10.1179/003258910X12827272082669

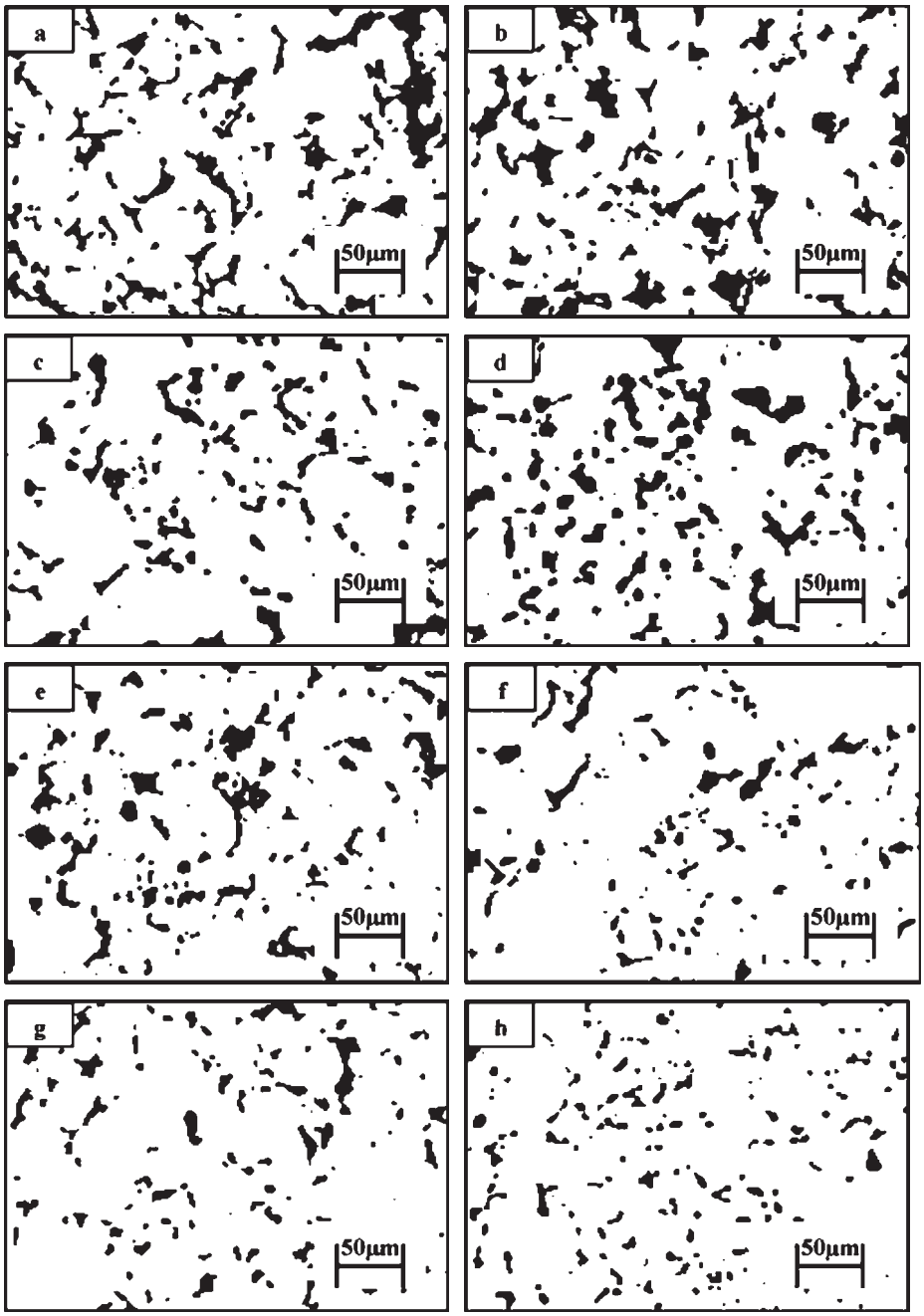

a as received, sintered; *b* prepassivated, sintered; *c* as received, annealed; *d* prepassivated, annealed; *e* as received, sintered; *f* prepassivated, sintered; *g* as received, annealed; *h* prepassivated, annealed

1 Micrographs of unetched 316L specimens in under *a–d* 500 MPa and *e–h* 700 MPa

with deionised water. Thereafter, the treated and as received powders were compacted as cylindrical specimens (10 mm in diameter and 13 mm in height) at 500 and 700 MPa. A matrix of 103·12 mm in diameter, 76·18 mm in height and 6 g of powder were used to make each specimen.

Compaction was carried out with floating die, without the use of a die lubricant. Green compacts were sintered in a vacuum furnace, reaching a vacuum of 10^{-3} mbar at 1200°C for 90 min and then cooled to 800°C under the vacuum atmosphere, and finally, the specimens were rapidly quenched in pure nitrogen atmosphere. Samples in these conditions were referred to as 'sintered specimens'. Half of the specimens were then annealed by heating at 1100°C for 300 min under a vacuum atmosphere before being water quenched. These were referred to as the 'annealed specimens'. After sintering, the density of the specimens was evaluated by water displacement method, based on Archimedes' principle (ASTM B328-03). Porosity features were also analysed by image analysis methods applied to optical microscopy images obtained from polished cross-sections of the samples. Ten images of different sections of the testpieces covering all the surfaces, obtained at a magnification of $\times 100$, were studied to obtain the values corresponding to each material.

The fraction of porosity was measured using conventional image analysis techniques and the CLEMEX software. The following parameter was measured individually for each pore to describe the stereological parameters of the pore structure and morphological characteristics.

D_{circle} is the diameter of the equivalent circle, i.e. the circle having the same area as the metallographic cross-section of the pore. Frequency distribution was used to estimate pore size and morphology.

Pore shape factor f_s is the determined profile irregularity of a pore, while pore elongation factor f_e represented the pore elongation

$$f_{shape} = 4\pi A/P^2 \quad (1)$$

where A and P are the area and perimeter of a pore

$$f_{elong} = D_{min}/D_{max} \quad (2)$$

where D_{min} and D_{max} are the minimum and the maximum Feret diameters of a pore respectively.

Frequency distribution was used to estimate pore size and morphology. For each parameter, the median value (the value at a cumulative frequency of 50%) was considered as the mean value.

For more precise microstructure examination, the prepassivated and as received powders were submitted to SEM observation, employing a SEM Leo model 1450. Feret average diameter and elongation factor were measured from several SEM images using image analysis technique. Frequency distribution and correlated median value were also used to evaluate the powder particles size and roundness.

Results and discussion

Figure 1 shows the unetched microstructure of materials as an example. Optical micrographs revealed different microstructures particularly in terms of pore size, morphology and distribution. The sample with the highest fraction of pores appeared to have much larger and more irregular pores than the other specimens. It could be seen that annealed specimens revealed more rounded pores without sharp corners on powder particles in comparison to sintered ones. Accordingly, annealed treatment reduced the irregularity of pores by providing sufficient time for atom migration and minimising surface ratio.

The area in the vicinity of pores with higher curvatures through irregularity in pore shape presented a higher vacancy concentration in equilibrium than the rounded pores with lower curvatures. The distance between different curvatures of irregularities in the same pore was smaller than the curvatures of pore geometry. Therefore, the evolution of pores to a spherical form was essentially accomplished by vacancies diffusion.

The porosity amount of the alloys is shown in Table 1. The porosity measured by Archimedes' method yielded values ranging from ~16% for 6·73 g cm^{-3} to 6% for 7·49 g cm^{-3}. These values were similar to the

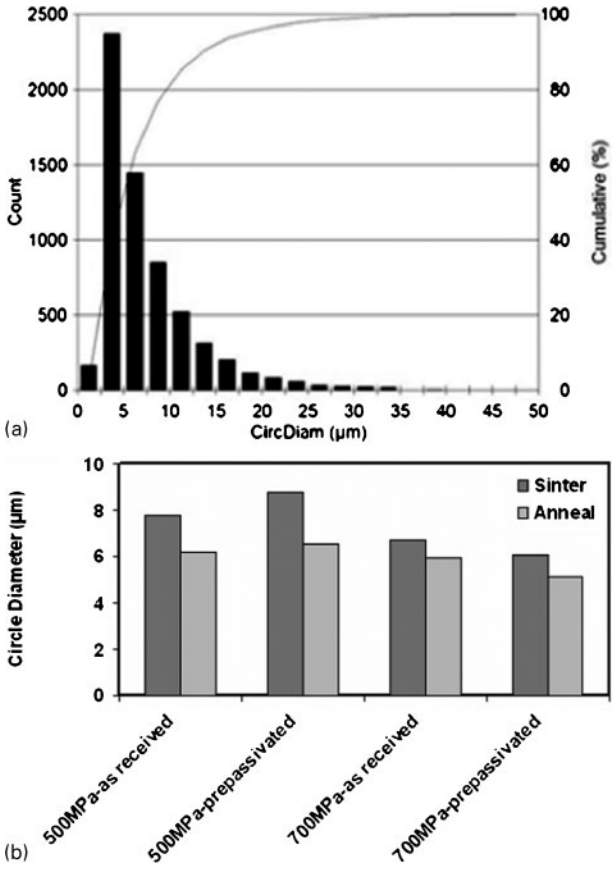

2 ***a*** **circle diameter and cumulative histogram of prepassivated specimen, compacted at 500 MPa and finally sintered as example and** ***b*** **median value of cumulative histogram for all specimens**

porosity values computed from the image analysis of alloys. To some extent, the lower fraction of surface porosity observed in all specimens in comparison to the similar total porosity was affiliated to the fact that the surface of some pores was closed off. Prepassivation reduced total and surface porosities, especially in the annealed specimens. It was proposed that prepassivation treatment reduced irregularity in powder particles through elimination of sharp corners of powder particles by exposure to acid environment. This phenomenon improved compressibility of prepassivated powder particles and reduced the diffusion paths.

Exposing the specimens to high temperatures for 300 min during annealed treatment encouraged the diffusion mechanism to minimise the pores, leading to reduction in the porosity fraction and increase in sintered density. As expected, total porosity and fraction of surface porosity decreased when compaction pressure

Table 1 Results of sintered density, pore number, total porosity and surface porosity of studied samples

Surface porosity, %	Total porosity, %	Pore number	Sintered density, g cm^{-3}	Sample
14·8	15·87	628	6·73	As received, 500 MPa, sintered
16·5	15·62	531	6·75	Prepassivated, 500 MPa, sintered
11·6	13·12	681	6·99	As received, 700 MPa, sintered
12·2	14·25	624	6·86	Prepassivated, 700 MPa, sintered
10·2	12·62	649	6·95	As received, 500 MPa, annealed
10·5	15·5	599	6·76	Prepassivated, 500 MPa, annealed
7·4	10·37	352	7·17	As received, 700 MPa, annealed
6·1	6·37	382	7·49	Prepassivated, 700 MPa, annealed

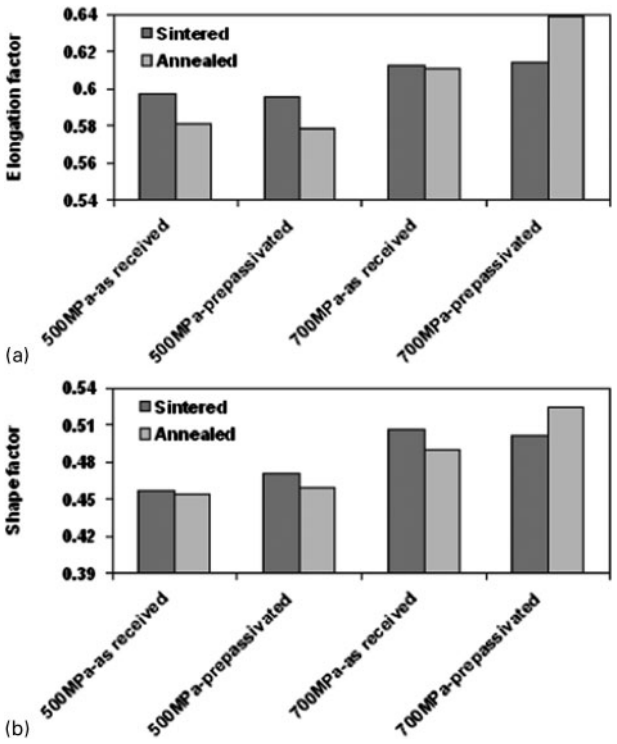

3 Cumulative frequency histograms of *a* elongation factor and *b* shape factor

increased. These results are reported in detail elsewhere.[8] In terms of pore count, it seemed that specimens with higher pore counts accompanying the lower area showed better properties. The highest sintered density (7·49 g cm^{-3}) was observed in the specimen with 700 MPa compact pressure, prepassivated in 20% nitric acid and finally annealed and was named the superior specimen.

Distribution of equivalent circle diameter of pores and the median value of cumulative histogram, shown in Fig. 2, as an example, revealed that annealed specimens had lower values than sintered ones. In addition, an increase in compaction pressure and prepassivation treatment, especially for those specimens compacted at high pressure, resulted in an evident reduction of pore diameter.

It could be observed that most pore diameters varied between 5 and 9 μm in the whole specimens ranging from 2 to 50 μm. The lowest pore diameter (with cumulative median values of 5·13 μm) was also observed in the superior specimen that was introduced before. It has been already approved that the addition of gas atomised powders to water atomised powders reduces pore diameter and pore size distribution.[15] A similar effect might have happened here due to prepassivation treatment in concentrated acid environment.

The corresponding cumulative frequency histograms and frequency distribution curves of elongation and

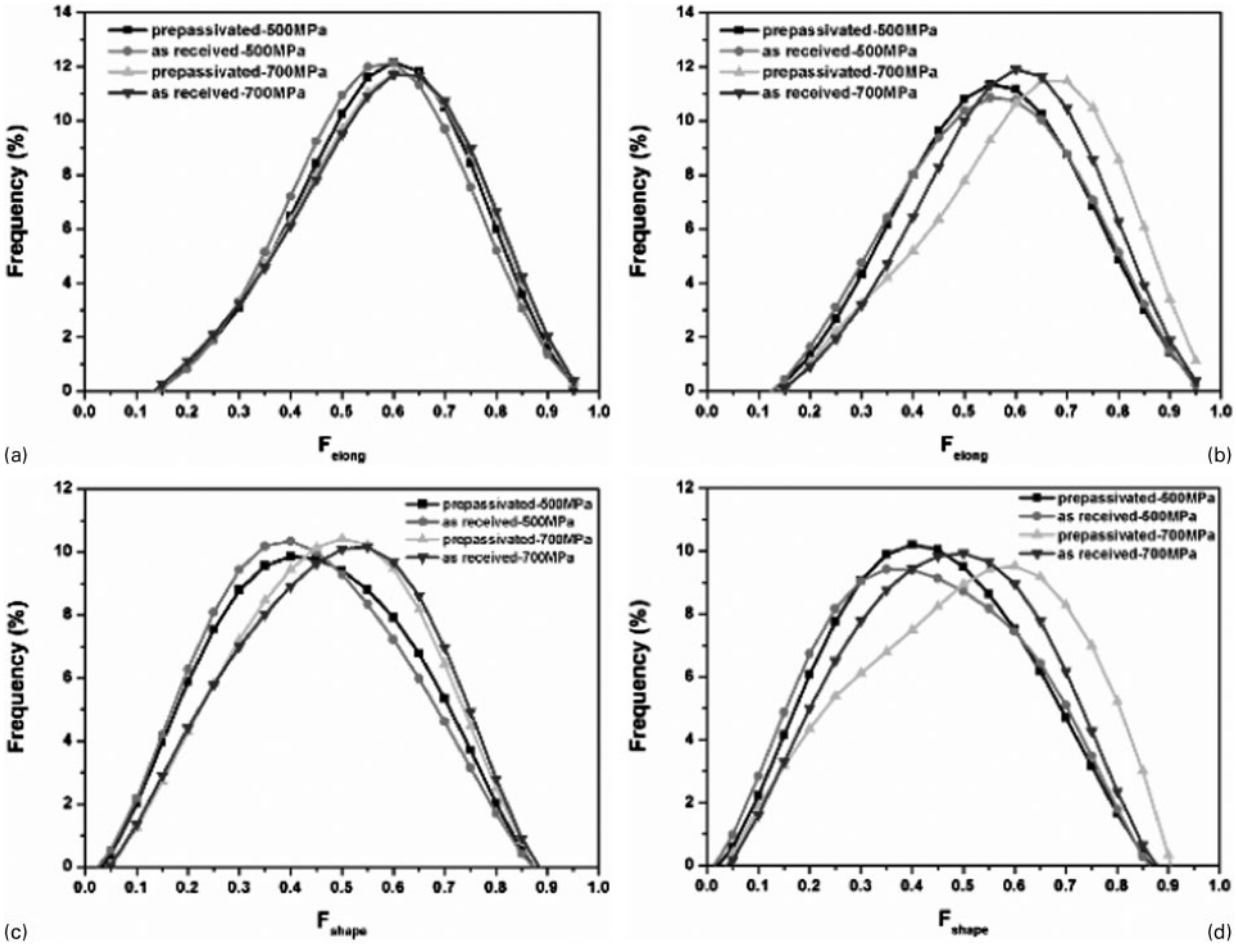

4 Frequency distribution curves versus *a* elongation factor of sintered, *b* elongation factor of annealed, *c* shape factor of sintered and *d* shaped factor of annealed specimens

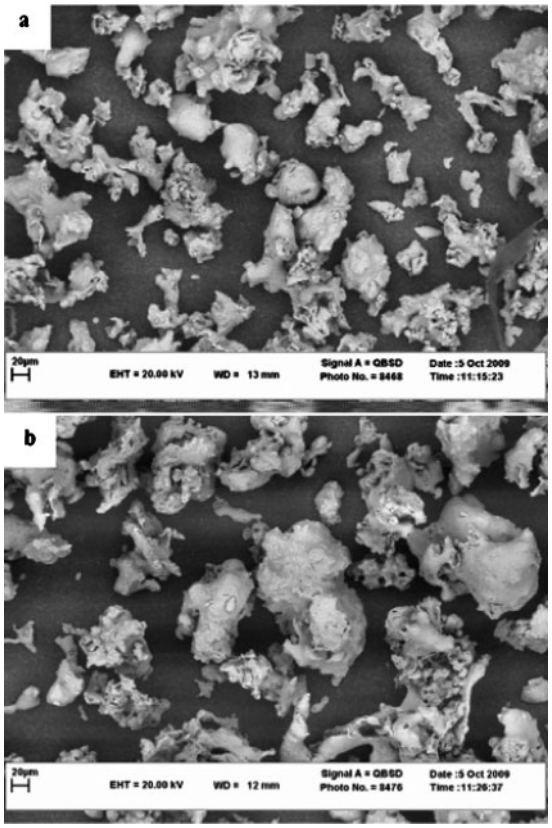

5 Images (SEM) of *a* prepassivated and *b* as received powder particles

shape factors are presented in Figs. 3 and 4 respectively. Generally, annealed specimen curves shifted towards higher values in comparison to sintered ones. In specimens compacted with 500 MPa, no significant changes were observed in shape and elongation factors between prepassivated and as received samples. In contrast, prepassivated specimens compacted at 700 MPa exhibited higher values of elongation and shape factors and were shifted towards higher values in comparison to as received ones. For the specimens applied with image analysis technique, as expected, elongation and shape factors increased when compaction pressure increased. Again, the highest roundness with 14% increase in f_{shape} and 9% increase in f_{elong} was observed in the superior specimen that was mentioned before. These results denoted an increase in the roundness of the prepassivated specimen's pores.

Images (SEM) of prepassivated and as received powder particles are shown in Fig. 5. The better circularity and lower Feret average diameter in prepassivated powder particles in comparison to the as received ones were quite evident. This confirmed the authors' previous observations and conclusions.

For a more accurate evaluation, further statistical assessment of powders was used. Figure 6 demonstrates the histograms of Feret average diameter versus distribution frequency for powder particles. It can be clearly noticed that the average Feret diameter decreased for prepassivated powder particles in comparison to as received ones by treating in nitric acid. A 21 μm reduction in the median value was also observed for Feret average diameter of prepassivated powder particles in comparison with the as received ones. In a more

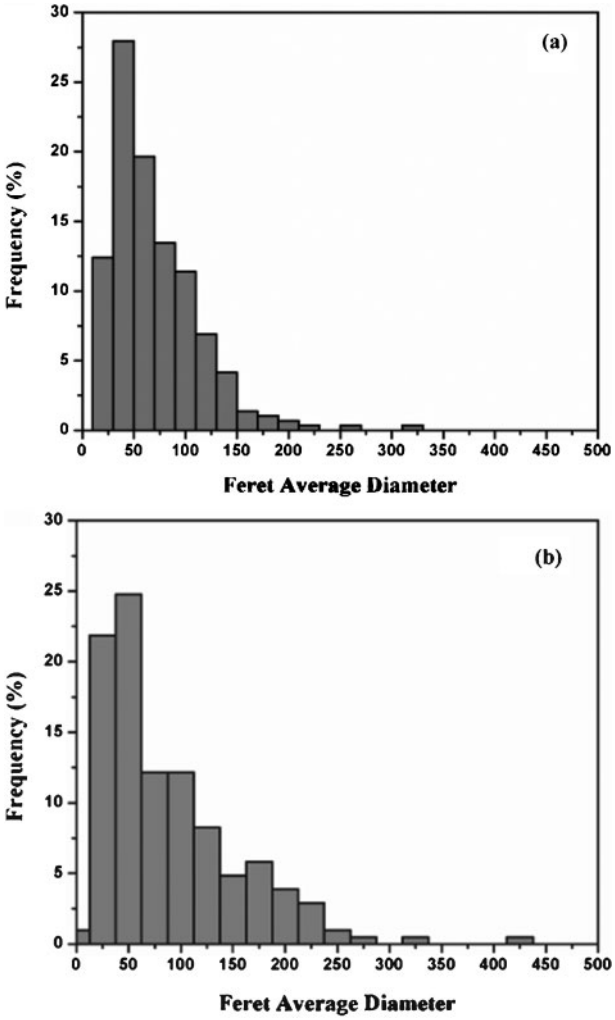

6 Histogram of Feret average diameters versus frequency for *a* prepassivated and *b* as received powder particles

detailed examination, the histogram of prepassivated powder particles revealed better uniformity than as received ones.

Frequency distribution of the elongation factor for prepassivated and as received powder particles are illustrated in Fig. 7. For prepassivated powder particles, the curve shifted towards higher value in compare with as received one. This indicates an increase in the

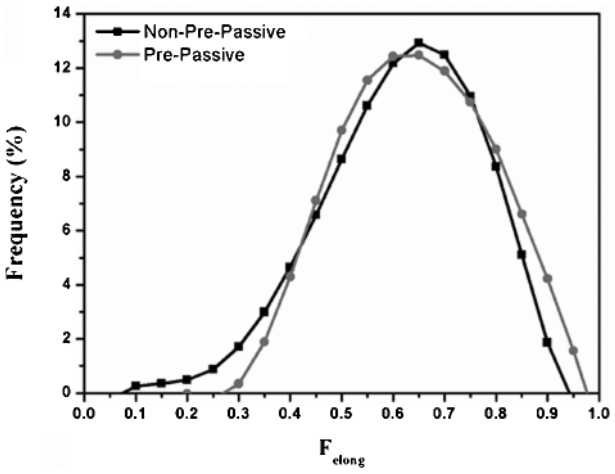

7 Frequency distribution curves of elongation factor for powder particles

roundness of prepassivated powder particles by elimination of sharp corners of powder particles during exposure to acid environment. A 3·2% increase in cumulative median value of elongation factor was observed for prepassivated powder particles. With accurate observation, it could be understood that the curve of prepassivated powder particles revealed better homogeneity than that of the as received one.

Conclusions

1. Increasing sintered density and compaction pressure accompanying with prepassivation treatment resulted in lower pore fraction and more spherical pore shape.

2. Reduction in equivalent circle diameter and increasing elongation and shape factors was observed in prepassivated specimens, particularly at higher compaction pressure, in comparison with as received ones.

3. The lowest pore diameter with 40% reduction in equivalent circle diameter and the highest roundness with 14% increase in f_{shape} and 9% increase in f_{elong} were observed in specimen with 700 MPa compact pressures, prepassivated in 20% nitric acid and finally annealed.

4. Statistical evaluation of the size and roundness of the prepassivated powder particles revealed that prepassivation had caused a 21 μm reduction in powder size and a 3·2% improvement in its roundness.

5. It was proposed that prepassivation treatment reduced irregularity and improved compressibility of powder particles through elimination of sharp corners of powder particles by exposure to acid environment.

Acknowledgements

The authors would like to appreciate the financial support from Ferdowsi University of Mashhad and provision of laboratory facilities during the period that this study was being carried out. The authors are grateful to Engineer Makarem and to the colleagues involved in the project for their contribution to this work.

References

1. E. Otero, A. Pardo, E. Saenz, M. V. Utrilla and P. Hierro: *Corros. Sci.*, 1996, **38**, 1485–1493.
2. T. Raghu, S. N. Malholtra and P. Ramakrisnan: *Br. Corros. J.*, 1988, **33**, 109–116.
3. E. Angelini, P. Bianco, F. Rosalbino, M. Rosso and G. Scavino: *Werkst. Korros.*, 1994, **45**, 392–401.
4. E. Otero, A. Pardo, E. Saenz, M. V. Utrilla and F. J. Álvarez: *Corros. Sci.*, 1998, **40**, 1421–1434.
5. A. Bautista, F. Velasco, S. Guzmán, D. de la Fuente, F. Cayuela and M. Morcillo: *Rev. Met.*, 2006, **42**, 175–184.
6. N. Tosangthum, O. Coovattanachi, R. Krataitong, M. Morakotjindo, A. Daraphan, B. Vetayanugul and R. Tongsri: *Chiang Mai J. Sci.*, 2006, **33**, 45–52.
7. B. Vetayanugul, O. Coovattanachai, R. Krataitong, R. Tongsri and P. Burke: Proc. 28th Congr. on 'Science and technology of Thailand', Bangkok, Thailand, October 2002, 637.
8. C. García, F. Martín, P. de Tiedra and L. García Cambronero: *Corros. Sci.*, 2007, **49**, 1718–1736.
9. H. C. Pavanati, A. M. Maliska, A. N. klein and L. R. Muzart: *Mater. Res.*, 2007, **10**, 87–93.
10. T. M. Puscas, M. Signorini, A. Molinari and G. Straffelini: *Mater. Charact.*, 2003, **50**, 1–10.
11. B. H. Kaye: in 'Particle shape characterization', (ed. P. W. Lee), Vol. 7, 605–617; 1998, Materials Park, OH, ASM International/ Laurentian University.
12. G. F. Bocchini, B. Rivolta, G. Silva, E. Poggio, M. R. Pinasco and M. G. Ienco: *Powder Metall.*, 2004, **47**, 343–351.
13. G. F. Bocchini, B. Rivolta and G. Silva: 'Various methods to assess the degree of sintering: a review', Proc. PM World Cong. 2007, Toulouse, France, October 2007, EPMA, 1–6/1658.
14. B. Shahabi Kargar, M. H. Moayed, A. Babakhani and A. Davoodi: *Corros. Sci.*, submitted.
15. C. Moral, A. Bautista and F. Velasco: *Corros. Sci.*, 2009, **51**, 1651–1657.